The 2013 World Congress on
Advances in Structural Engineering and Mechanics (ASEM13)
Jeju, Korea, September 8-12, 2013

Three-Dimensional Elastic Analysis of Orthotropic Plates by using Element-Free Galerkin Method

*Yoshitaka Suetake[1)]

[1)] *Division of Architecture and Civil Engineering, Ashikaga Institute of Technology, Ashikaga 326-8558, Japan*
[1)] ysuetake@ashitech.ac.jp

ABSTRACT

In this investigation, a three-dimensional elastic analysis of orthotropic plates is performed by using an element-free Galerkin method (EFGM). Especially, the Lagrange polynomial is employed here for the discretization.

On the other hand, a Fourier analysis is also employed for the analysis of orthotropic plates for comparison. In the present Fourier analysis, we can simply establish general solutions which involve 6 arbitrary constants, which can be determined completely by using traction boundary conditions on the upper and the lower surfaces of the plates.

Several numerical examples are presented in order to demonstrate the efficiency of the present EFGM. As an example, we adopt here simply supported rectangular plates and evaluate in-plane displacement and transverse shear stress distributions along the thickness of plates. It follows from the numerical results that relatively good approximation is obtained by using the present EFGM.

1. INTRODUCTION

Many research works on the Element-Free Galerkin Method (EFGM) have been presented in solid mechanics. Since EFGM does not require the finite element subdivision, it draws the attention of engineers as an alternative numerical approach for solving partial differential equations. The EFGM is introduced by Belytshko et al. (1994), who refined and modified the Diffused Element Method (DFM) presented by Nayroles et al. (1992). Both EFGM and DFM are based on the moving least squares (MLS) approximation by Lancaster and Salkauskas (1981). The author also proposes a simple element free approach (2002) in which the Lagrange polynomial is employed. The simple element free method is not based on MLS and can connect an approximate solution and its derivatives directly with nodal values.

On the other hand, three-dimensional anisotropic elastic behaviors of plates are also investigated by many authors, for example, Pagano (1970), Srinivas and Rao (1970),

[1)] Professor

Wittrick (1987), Kaprielian et al. (1988), Mian and Spencer (1998), Tabakov (2005), Chang and Tarn (2012). In those investigations, three-dimensional elastic analyses of orthotropic thick plates and laminates are dealt with. Especially, three-dimensional exact solutions for orthotropic rectangular plates are presented and the bending, vibration and buckling problems of simply supported plates and laminates are discussed in those research works.

In this investigation, a three-dimensional elastic analysis of orthotropic plates is performed by using the simple element-free approach, in which the Lagrange polynomial is employed for the discretization. In addition, a Fourier analysis is also employed for the analysis of orthotropic plates for comparison. In the present Fourier analysis, we can simply establish general solutions which involve 6 arbitrary constants, which can be determined completely by using traction boundary conditions on the upper and the lower surfaces of the plates.

Several numerical examples are presented in order to demonstrate the efficiency of the present EFGM. As an example, we adopt here simply supported rectangular plates. In-plane displacement and transverse shear stress distributions along the thickness of plates are calculated by both approaches. It follows from the numerical results that relatively good approximation can be obtained by using the present EFGM.

2. EFGM BY USING LAGRANGE POLYNOMIALS

In a numerical analysis, we have to establish a discretization scheme, in which an approximate solution is represented by discrete data. Interpolation gives us one of such schemes. In the finite element methods, for example, interpolation is performed within each element. On the other hand, in EFGM, an approximate solution at an arbitrary point is calculated from carefully selected nodal values. The nodal points can be selected in a neighborhood of the point at which the approximate solution is calculated. The neighborhood of the point does not always mean a finite element. It is sufficient that the neighborhood is set around each solution point. Namely, the approximate solution can be represented by nodal values without a finite element. In the present investigation, the Lagrange polynomial is employed for the connection of an arbitrary point value to nodal ones.

2.1. Formulation in One-Dimensional Region

For a given set $\{x_i\}(i=0\sim N)$ of $N+1$ nodal points in a one-dimensional region, the basis of the Lagrange polynomial can be written as

$$\varphi_i(x)=\prod_{m=0}^{N} X_{m,i}(x) \quad ; \quad X_{m,i}(x)=\frac{x-x_m}{x_i-x_m}\ (m\neq i) \quad , \quad 1\ (m=i)\,. \tag{1}$$

Note that the Lagrange basis is characterized by $\varphi_i(x_j)=\delta_{ij}$, where δ_{ij} is the Kronecker's delta. By using the Lagrange basis, we can interpolate the discrete data $f_i(i=0\sim N)$ at the nodal points x_i as

$$f(x) = \sum_{i=0}^{N} f_i \varphi_i(x), \tag{2}$$

which is the so-called Lagrange polynomial. Equation (2) satisfies the matching condition $f(x_i) = f_i$.

The Lagrange polynomial (2) can be employed as a tool connecting a value at an arbitrarily fixed point x with the nodal values $f_i (i = 0 \sim N)$ around x. The nodal points can be selected in a neighborhood of the point x, for example, a ρ-neighborhood Ω, $(x-\rho, x+\rho)$. Then the approximate solution and its derivatives at x can be represented by the nodal values f_i in Ω. In what follows, such a point x is called "an evaluation point" and such a neighborhood Ω "a support region", the size of which is prescribed by "the support parameter" ρ. Although each element itself can be interpreted as a fixed support region in the finite element method, the support region in the EFGM moves with the evaluation point.

2.2. Formulation in Three-Dimensional Region

In three-dimensional problems, we can also employ the Lagrange polynomial for the EFGM discretization. We can define the three-dimensional Lagrange polynomial by using the one-dimensional Lagrange bases as follows. If $(N+1)^3$ nodal points $(x_i, y_j, z_k)(i, j, k = 0 \sim N)$ are distributed as lattice points, we can interpolate the discrete data f_{ijk} at the nodal points (x_i, y_j, z_k) as

$$f(x, y, z) = \sum_{k=0}^{N} \sum_{j=0}^{N} \sum_{i=0}^{N} f_{ijk} \varphi_i(x) \psi_j(y) \omega_k(z), \tag{3}$$

in which $\varphi_i(x)$, $\psi_j(y)$, and $\omega_k(z)$ are the one-dimensional Lagrange bases defined as Eq. (1). Equation (3) satisfies the matching condition $f(x_i, y_j, z_k) = f_{ijk}$ again. Then the support region Ω near the evaluation point (x, y, z) is a cube with a side length 2ρ as shown in Fig. 1.

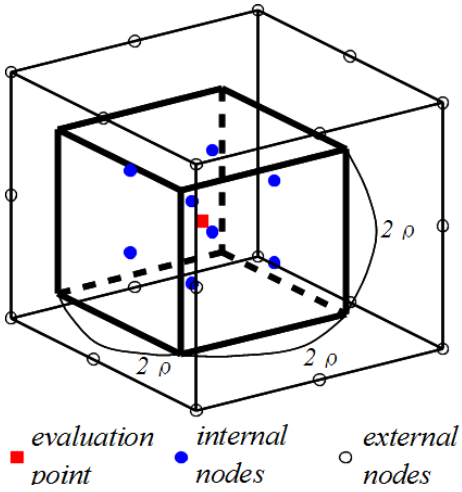

Fig. 1. Three-dimensional support region.

By using the three-dimensional Lagrange polynomial (3), the following vector expression of the approximate solution and its first derivatives at the evaluation point (x, y, z):

$$f(x,y) = \boldsymbol{B}_0(x,y)^T.\boldsymbol{f} \quad , \quad \frac{\partial f}{\partial x} = \boldsymbol{B}_1(x,y)^T.\boldsymbol{f} \quad , \quad \frac{\partial f}{\partial y} = \boldsymbol{B}_2(x,y)^T.\boldsymbol{f} \quad , \quad \frac{\partial f}{\partial z} = \boldsymbol{B}_3(x,y)^T.\boldsymbol{f} \ , \quad (4)$$

where

$$\begin{cases} \boldsymbol{B}_0(x,y)^T = \lfloor \varphi_0(x)\psi_0(y)\omega_0(z)\cdots\varphi_i(x)\psi_j(y)\omega_k(z)\cdots\varphi_N(x)\psi_N(y)\omega_N(z) \rfloor \\ \boldsymbol{B}_1(x,y)^T = \lfloor \varphi_0^{(1)}(x)\psi_0(y)\omega_0(z)\cdots\varphi_i^{(1)}(x)\psi_j(y)\omega_k(z)\cdots\varphi_N^{(1)}(x)\psi_N(y)\omega_N(z) \rfloor \\ \boldsymbol{B}_2(x,y)^T = \lfloor \varphi_0(x)\psi_0^{(1)}(y)\omega_0(z)\cdots\varphi_i(x)\psi_j^{(1)}(y)\omega_k(z)\cdots\varphi_N(x)\psi_N^{(1)}(y)\omega_N(z) \rfloor \\ \boldsymbol{B}_3(x,y)^T = \lfloor \varphi_0(x)\psi_0(y)\omega_0^{(1)}(z)\cdots\varphi_i(x)\psi_j(y)\omega_k^{(1)}(z)\cdots\varphi_N(x)\psi_N(y)\omega_N^{(1)}(z) \rfloor \end{cases}, \quad (5)$$

and

$$\boldsymbol{f}^T = \lfloor f_{000} \quad f_{001}\cdots f_{00N} \quad f_{010}\, f_{011}\cdots f_{01N} \quad f_{020}\cdots f_{ijk}\cdots f_{NNN} \rfloor, \quad (6)$$

When using Eq. (4), we can obtain the element-free discretization procedure for 3-D problems.

2.3. Variational Formulation for Three-Dimensional Orthotropic Bodies

The principle of virtual work for 3-D bodies is given by

$$\iiint_V (\sigma_x \delta\varepsilon_x + \sigma_y \delta\varepsilon_y + \sigma_z \delta\varepsilon_z + \tau_{xy}\delta\gamma_{xy} + \tau_{yz}\delta\gamma_{yz} + \tau_{xz}\delta\gamma_{xz})dxdydz$$
$$- \iiint_V (\bar{X}\delta U + \bar{Y}\delta V + \bar{Z}\delta W)dxdydz - \iint_{S_\sigma} (\bar{T}_x \delta U + \bar{T}_y \delta V + \bar{T}_z \delta W)dS = 0 \quad , \tag{7}$$

where (U,V,W) are displacements in the x-, the y-, and the z-directions, σ and τ mean normal and shear stresses, ε and γ mean normal and shear strains, $(\bar{X},\bar{Y},\bar{Z})$ are body forces, and $(\bar{T}_x,\bar{T}_y,\bar{T}_z)$ are surface tractions in the three directions.

Discretized representations of displacements and strains are as follows:

$$U = \boldsymbol{B}_0^{\,T}.\boldsymbol{U} \quad , \quad V = \boldsymbol{B}_0^{\,T}.\boldsymbol{V} \quad , \quad W = \boldsymbol{B}_0^{\,T}.\boldsymbol{W} \, , \tag{8}$$

$$\begin{cases} \varepsilon_x = \dfrac{\partial u}{\partial x} = \boldsymbol{B}_1^{\,T}.\boldsymbol{u} \quad , \quad \varepsilon_y = \dfrac{\partial v}{\partial y} = \boldsymbol{B}_2^{\,T}.\boldsymbol{v} \quad , \quad \varepsilon_z = \dfrac{\partial w}{\partial z} = \boldsymbol{B}_3^{\,T}.\boldsymbol{w} \\ \gamma_{xy} = (\dfrac{\partial u}{\partial y} + \dfrac{\partial v}{\partial x}) = \boldsymbol{B}_2^{\,T}.\boldsymbol{u} + \boldsymbol{B}_1^{\,T}.\boldsymbol{v} \quad , \quad \gamma_{yz} = \boldsymbol{B}_3^{\,T}.\boldsymbol{v} + \boldsymbol{B}_2^{\,T}.\boldsymbol{w} \quad , \quad \gamma_{zx} = \boldsymbol{B}_1^{\,T}.\boldsymbol{w} + \boldsymbol{B}_3^{\,T}.\boldsymbol{u} \end{cases} . \tag{9}$$

Hooke's law for orthotropic materials are given by

$$\begin{Bmatrix} \sigma_x \\ \sigma_y \\ \sigma_z \\ \tau_{xy} \\ \tau_{yz} \\ \tau_{zx} \end{Bmatrix} = \frac{E}{\tilde{N}} \begin{bmatrix} \hat{C}_{xx} & \hat{C}_{xy} & \hat{C}_{zx} & 0 & 0 & 0 \\ \hat{C}_{xy} & \hat{C}_{yy} & \hat{C}_{yz} & 0 & 0 & 0 \\ \hat{C}_{zx} & \hat{C}_{yz} & \hat{C}_{zz} & 0 & 0 & 0 \\ 0 & 0 & 0 & \beta_{xy} & 0 & 0 \\ 0 & 0 & 0 & 0 & \beta_{yz} & 0 \\ 0 & 0 & 0 & 0 & 0 & \beta_{zx} \end{bmatrix} \begin{Bmatrix} \varepsilon_x \\ \varepsilon_y \\ \varepsilon_z \\ \gamma_{xy} \\ \gamma_{yz} \\ \gamma_{zx} \end{Bmatrix} , \tag{10}$$

where E is a standard value of Young's modulus and

$$\begin{cases} \hat{C}_{xx} \equiv \alpha_x(1-\nu_{yz}\nu_{zy}) \quad , \quad \hat{C}_{yy} \equiv \alpha_y(1-\nu_{zx}\nu_{xz}) \quad , \quad \hat{C}_{zz} \equiv \alpha_z(1-\nu_{xy}\nu_{yx}) \quad , \\ \hat{C}_{xy} = \hat{C}_{yx} \equiv \alpha_x(\nu_{yx}+\nu_{yz}\nu_{zx}) \; , \; \hat{C}_{yz} = \hat{C}_{zy} \equiv \alpha_y(\nu_{zy}+\nu_{zx}\nu_{xy}) \; , \; \hat{C}_{zx} = \hat{C}_{xz} \equiv \alpha_z(\nu_{xz}+\nu_{xy}\nu_{yz}) \; , \, , \\ \tilde{N} \equiv 1-\nu_{xy}\nu_{yx}-\nu_{yz}\nu_{zy}-\nu_{zx}\nu_{xz}-2\nu_{xy}\nu_{yz}\nu_{zx} \quad ; \quad \alpha_x \equiv \dfrac{E_x}{E} \quad , \alpha_y \equiv \dfrac{E_y}{E} \quad , \quad \alpha_z \equiv \dfrac{E_z}{E} \end{cases} \tag{11}$$

and

$$\beta_{xy} \equiv \frac{\tilde{N}G_{xy}}{E} \quad , \quad \beta_{yz} \equiv \frac{\tilde{N}G_{yz}}{E} \quad , \quad \beta_{zx} \equiv \frac{\tilde{N}G_{zx}}{E} \, . \tag{12}$$

In Eq. (11) and Eq. (12), ν means Poisson's ratios and G Shear moduli. For example, ν_{xy} is a Poisson's ratio in the x-y plane and G_{yz} is a shear modulus in the y-z plane. Note that the following reciprocal relations are derived from symmetry of the strain-stress relation:

$$\frac{\nu_{xy}}{E_x}=\frac{\nu_{yx}}{E_y} \quad , \quad \frac{\nu_{xz}}{E_x}=\frac{\nu_{zx}}{E_z} \quad , \quad \frac{\nu_{yz}}{E_y}=\frac{\nu_{zy}}{E_z} \quad or \quad \frac{\nu_{xy}}{\alpha_x}=\frac{\nu_{yx}}{\alpha_y} \quad , \quad \frac{\nu_{xz}}{\alpha_x}=\frac{\nu_{zx}}{\alpha_z} \quad , \quad \frac{\nu_{yz}}{\alpha_y}=\frac{\nu_{zy}}{\alpha_z} . \quad (13)$$

Substitution of Eq. (8) and Eq. (9) into Eq. (7), in view of Eq. (10), gives us the following discretized governing equation for three-dimensional elastic problems of orthotropic bodies:

$$\begin{bmatrix} \boldsymbol{K}_{11} & \boldsymbol{K}_{12} & \boldsymbol{K}_{13} \\ \boldsymbol{K}_{21} & \boldsymbol{K}_{22} & \boldsymbol{K}_{23} \\ \boldsymbol{K}_{31} & \boldsymbol{K}_{32} & \boldsymbol{K}_{33} \end{bmatrix} \begin{Bmatrix} \boldsymbol{U} \\ \boldsymbol{V} \\ \boldsymbol{W} \end{Bmatrix} = \begin{Bmatrix} \boldsymbol{F}_x \\ \boldsymbol{F}_y \\ \boldsymbol{F}_z \end{Bmatrix}, \quad (14)$$

where

$$\begin{cases} \boldsymbol{K}_{11} \equiv \frac{E_x}{\tilde{N}} \iiint_V (\hat{C}_{xx}\boldsymbol{B}_1\boldsymbol{B}_1^T + \beta_{xy}\boldsymbol{B}_2\boldsymbol{B}_2^T + \beta_{xz}\boldsymbol{B}_3\boldsymbol{B}_3^T)dxdydz \\ \boldsymbol{K}_{22} \equiv \frac{E_x}{\tilde{N}} \iiint_V (\beta_{xy}\boldsymbol{B}_1\boldsymbol{B}_1^T + \hat{C}_{yy}\boldsymbol{B}_2\boldsymbol{B}_2^T + \beta_{yz}\boldsymbol{B}_3\boldsymbol{B}_3^T)dxdydz \\ \boldsymbol{K}_{33} \equiv \frac{E_x}{\tilde{N}} \iiint_V (\beta_{yz}\boldsymbol{B}_2\boldsymbol{B}_2^T + \beta_{xz}\boldsymbol{B}_1\boldsymbol{B}_1^T + \hat{C}_{zz}\boldsymbol{B}_3\boldsymbol{B}_3^T)dxdydz \\ \boldsymbol{K}_{12} = \boldsymbol{K}_{21}^T \equiv \frac{E_x}{\tilde{N}} \iiint_V (\hat{C}_{xy}\boldsymbol{B}_1\boldsymbol{B}_2^T + \beta_{xy}\boldsymbol{B}_2\boldsymbol{B}_1^T)dxdydz \\ \boldsymbol{K}_{23} = \boldsymbol{K}_{32}^T \equiv \frac{E_x}{\tilde{N}} \iiint_V (\hat{C}_{yz}\boldsymbol{B}_2\boldsymbol{B}_3^T + \beta_{yz}\boldsymbol{B}_3\boldsymbol{B}_2^T)dxdydz \\ \boldsymbol{K}_{31} = \boldsymbol{K}_{13}^T \equiv \frac{E_x}{\tilde{N}} \iiint_V (\hat{C}_{xz}\boldsymbol{B}_3\boldsymbol{B}_1^T + \beta_{xz}\boldsymbol{B}_1\boldsymbol{B}_3^T)dxdydz \end{cases} , \quad \begin{cases} \boldsymbol{F}_x \equiv \iiint_V \bar{F}_x\boldsymbol{B}_0 dxdydz + \iint_{S_\sigma} \bar{T}_x\underline{\boldsymbol{B}}_0 dS \\ \boldsymbol{F}_y \equiv \iiint_V \bar{F}_y\boldsymbol{B}_0 dxdydz + \iint_{S_\sigma} \bar{T}_y\underline{\boldsymbol{B}}_0 dS , \\ \boldsymbol{F}_z \equiv \iiint_V \bar{F}_z\boldsymbol{B}_0 dxdydz + \iint_{S_\sigma} \bar{T}_z\underline{\boldsymbol{B}}_0 dS \end{cases}$$

(15), (16)

The integration in the above expressions is evaluated with the Gaussian quadrature formula and Gauss points are regarded as the evaluation points in the present element -free procedure. For the refinement of the integration accuracy, the global plate domain is divided into several sub-domains called "cells". The Gaussian quadrature formula is applied to the integration within each cell. We should note that the cell is not a finite element since the generation of cells is independent of the node distribution.

3. FOURIER ANALYSIS OF ORTHOTROPIC PLATES

In this section, a Fourier analysis of plates is explained, in which the plates are regarded as three-dimensional orthotropic bodies. Plate models treated here are simply supported rectangular plates.

3.1. Governing Equations

Substituting Eq. (10) into the equilibrium equations of 3-D bodies, in view of the strain-displacement relations, we have the following governing equations for orthotropic elastic bodies:

$$\begin{cases} (\hat{C}_{xx}\dfrac{\partial^2}{\partial x^2}+\beta_{xy}\dfrac{\partial^2}{\partial y^2}+\beta_{zx}\dfrac{\partial^2}{\partial z^2})U+(\hat{C}_{xy}+\beta_{xy})\dfrac{\partial^2 V}{\partial x\partial y}+(\hat{C}_{zx}+\beta_{zx})\dfrac{\partial^2 W}{\partial z\partial x}=0 \\ (\beta_{xy}\dfrac{\partial^2}{\partial x^2}+\hat{C}_{yy}\dfrac{\partial^2}{\partial y^2}+\beta_{yz}\dfrac{\partial^2}{\partial z^2})V+(\hat{C}_{xy}+\beta_{xy})\dfrac{\partial^2 U}{\partial x\partial y}+(\hat{C}_{yz}+\beta_{yz})\dfrac{\partial^2 W}{\partial y\partial z}=0 \\ (\beta_{zx}\dfrac{\partial^2}{\partial x^2}+\beta_{yz}\dfrac{\partial^2}{\partial y^2}+\hat{C}_{zz}\dfrac{\partial^2}{\partial z^2})W+(\hat{C}_{zx}+\beta_{zx})\dfrac{\partial^2 U}{\partial z\partial x}+(\hat{C}_{yz}+\beta_{yz})\dfrac{\partial^2 V}{\partial y\partial z}+\dfrac{\tilde{N}}{Et}\bar{p}_0=0 \end{cases} . \quad (17)$$

where t is a thickness of plates, only the body force in the z-direction $\bar{p}_0/t$, which is constant, is considered and the body forces in the other two directions are ignored. The body force considered here corresponds to, for example, a dead load of plates. Note that the body force is usually ignored in the previous investigations.

3.2. General Solutions

Since fully simply-supported plates are dealt with in this paper, the displacements in the three directions can be expressed as the following trigonometric series:

$$\begin{cases} U=\sum_k\sum_j U_{jk}(z)\cos\lambda_j x\sin\mu_k y \\ V=\sum_k\sum_j V_{jk}(z)\sin\lambda_j x\cos\mu_k y \\ W=\sum_k\sum_j W_{jk}(z)\sin\lambda_j x\sin\mu_k y \end{cases} ; \quad \lambda_j\equiv\frac{j\pi}{a}, \quad \mu_k\equiv\frac{k\pi}{b}. \quad (18)$$

The displacement field (18) satisfies the following geometrical boundary conditions a priori:

$$\begin{cases} U(x,0,z)=U(x,b,z)=0\,,\ V(0,y,z)=V(a,y,z)=0 \\ W(0,y,z)=W(a,y,z)=W(x,0,z)=W(x,b,z)=0 \end{cases} . \quad (19)$$

Substituting Eq. (18) into Eq. (17), we have the simultaneous ordinary differential equations for determining $U_{jk}(z)$, $V_{jk}(z)$, and $W_{jk}(z)$:

$$\begin{cases} (\beta_{zx}d^2 - {}_1\kappa_{jk}{}^2)U_{jk} - (\hat{C}_{xy} + \beta_{xy})\lambda_j\mu_k V_{jk} + (\hat{C}_{zx} + \beta_{zx})\lambda_j dW_{jk} = 0 \\ (\beta_{yz}d^2 - {}_2\kappa_{jk}{}^2)V_{jk} - (\hat{C}_{xy} + \beta_{xy})\lambda_j\mu_k U_{jk} + (\hat{C}_{yz} + \beta_{yz})\mu_k dW_{jk} = 0 \\ (\hat{C}_{zz}d^2 - {}_3\kappa_{jk}{}^2)W_{jk} - (\hat{C}_{zx} + \beta_{zx})\lambda_j dU_{jk} - (\hat{C}_{yz} + \beta_{yz})\mu_k dV_{jk} + \dfrac{\tilde{N}}{Et}\overline{P}_{jk}^{(0)} = 0 \end{cases}, \quad (20)$$

where

$$d \equiv \frac{d}{dz} \quad , \quad {}_1\kappa_{jk}{}^2 \equiv \hat{C}_{xx}\lambda_j{}^2 + \beta_{xy}\mu_k{}^2 \quad , \quad {}_2\kappa_{jk}{}^2 \equiv \beta_{xy}\lambda_j{}^2 + \hat{C}_{yy}\mu_k{}^2 \quad , \quad {}_3\kappa_{jk}{}^2 \equiv \beta_{zx}\lambda_j{}^2 + \beta_{yz}\mu_k{}^2 \,. \quad (21)$$

In order to obtain complementary solutions of Eq. (20), a characteristic equation is derived as

$$\begin{vmatrix} \beta_{zx}d^2 - {}_1\kappa_{jk}{}^2 & -(\hat{C}_{xy} + \beta_{xy})\lambda_j\mu_k & (\hat{C}_{zx} + \beta_{zx})\lambda_j d \\ -(\hat{C}_{xy} + \beta_{xy})\lambda_j\mu_k & \beta_{yz}d^2 - {}_2\kappa_{jk}{}^2 & (\hat{C}_{yz} + \beta_{yz})\mu_k d \\ -(\hat{C}_{zx} + \beta_{zx})\lambda_j d & -(\hat{C}_{yz} + \beta_{yz})\mu_k d & \hat{C}_{zz}d^2 - {}_3\kappa_{jk}{}^2 \end{vmatrix} = 0 \,. \quad (21)$$

Since this characteristic equation is a cubic equation with respect to d^2, the roots of it are easily found through the cubic formula.

It is assumed here that the characteristic equation (21) has 6 deferent roots, that is, characteristic values $d = \pm\rho_{jk}^{(i)}$ $(i = 1 \sim 3)$. By using these characteristic values, we can obtain a general solution set for $U_{jk}(z)$, $V_{jk}(z)$, and $W_{jk}(z)$ as

$$\begin{cases} U_{jk}(z) = \sum_{i=1}^{3} \dfrac{A_{31}^{(i)}}{A_{33}^{(i)}}(C_{jk}^{(i)} \cosh \rho_{jk}^{(i)} z + D_{jk}^{(i)} \sinh \rho_{jk}^{(i)} z) \\ V_{jk}(z) = \sum_{i=1}^{3} \dfrac{A_{32}^{(i)}}{A_{33}^{(i)}}(C_{jk}^{(i)} \cosh \rho_{jk}^{(i)} z + D_{jk}^{(i)} \sinh \rho_{jk}^{(i)} z) \\ W_{jk}(z) = \sum_{i=1}^{3} (C_{jk}^{(i)} \sinh \rho_{jk}^{(i)} z + D_{jk}^{(i)} \cosh \rho_{jk}^{(i)} z) + \dfrac{\tilde{N}\overline{P}_{jk}^{(0)}}{E_x t\, {}_3\kappa_{jk}{}^2} \end{cases} . \quad (22)$$

In Eq. (22), the parameters $A_{jk}^{(i)}$ are cofactors corresponding to the characteristic values $\rho_{jk}^{(i)}$ and they are given by

$$\begin{cases} A_{31}^{(i)} = -\lambda_j \rho_{jk}^{(i)} \{(\hat{C}_{zx} + \beta_{zx})(\beta_{yz}\rho_{jk}^{(i)2} - {}_2\kappa_{jk}{}^2) + (\hat{C}_{xy} + \beta_{xy})(\hat{C}_{yz} + \beta_{yz})\mu_k{}^2\} \\ A_{32}^{(i)} = -\mu_k \rho_{jk}^{(i)} \{(\hat{C}_{yz} + \beta_{yz})(\beta_{zx}\rho_{jk}^{(i)2} - {}_1\kappa_{jk}{}^2) + (\hat{C}_{xy} + \beta_{xy})(\hat{C}_{zx} + \beta_{zx})\lambda_j{}^2\} \\ A_{33}^{(i)} = (\beta_{zx}\rho_{jk}^{(i)2} - {}_1\kappa_{jk}{}^2)(\beta_{yz}\rho_{jk}^{(i)2} - {}_2\kappa_{jk}{}^2) - (\hat{C}_{xy} + \beta_{xy})^2 \lambda_j{}^2 \mu_k{}^2 \end{cases} . \quad (23)$$

The general solution (22) includes 6 arbitrary constants $C_{jk}^{(i)}$ $(i=1\sim 3)$ and $D_{jk}^{(i)}$, which are determined by applying the traction boundary conditions on the upper and lower surfaces of plates.

3.3. Traction Boundary Conditions

The 6 arbitrary constants $C_{jk}^{(i)}$ and $D_{jk}^{(i)}$ are determined by applying the traction boundary conditions on the upper and lower surfaces of plates. Those traction boundary conditions are given by

$$\begin{cases} \sigma_z(x,y,-\dfrac{t}{2}) = -\bar{p}_1(x,y) \\ \sigma_z(x,y,\dfrac{t}{2}) = \bar{p}_2(x,y) \\ \tau_{xz}(x,y,\pm\dfrac{t}{2}) = \tau_{yz}(x,y,\pm\dfrac{t}{2}) = 0 \end{cases} . \tag{24}$$

By using these 6 boundary conditions, we can determine the 6 arbitrary constants $C_{jk}^{(i)}$ and $D_{jk}^{(i)}$ as

$$C_{jk}^{(1)} = \frac{1}{det_1}(a_{12}a_{23} - a_{13}a_{22})sh_{jk}^{(2)}sh_{jk}^{(3)}\bar{R}_{jk}, \tag{25}$$

$$C_{jk}^{(2)} = -\frac{1}{det_1}(a_{11}a_{23} - a_{13}a_{21})sh_{jk}^{(1)}sh_{jk}^{(3)}\bar{R}_{jk}, \tag{26}$$

$$C_{jk}^{(3)} = \frac{1}{det_1}(a_{11}a_{22} - a_{12}a_{21})sh_{jk}^{(1)}sh_{jk}^{(2)}\bar{R}_{jk}, \tag{27}$$

$$\begin{aligned} D_{jk}^{(1)} = \frac{1}{det_2}\{&(a_{12}a_{23} - a_{13}a_{22})ch_{jk}^{(2)}ch_{jk}^{(3)}\bar{S}_{jk} - (a_{22}a_{33}ch_{jk}^{(2)}sh_{jk}^{(3)} - a_{23}a_{32}sh_{jk}^{(2)}ch_{jk}^{(3)})\lambda_j\bar{Q}_{jk} \\ &+ (a_{12}a_{33}ch_{jk}^{(2)}sh_{jk}^{(3)} - a_{13}a_{32}sh_{jk}^{(2)}ch_{jk}^{(3)})\mu_k\bar{Q}_{jk}\}, \end{aligned} \tag{28}$$

$$\begin{aligned} D_{jk}^{(2)} = -\frac{1}{det_2}\{&(a_{11}a_{23} - a_{13}a_{21})ch_{jk}^{(1)}ch_{jk}^{(3)}\bar{S}_{jk} - (a_{21}a_{33}ch_{jk}^{(1)}sh_{jk}^{(3)} - a_{23}a_{31}sh_{jk}^{(1)}ch_{jk}^{(3)})\lambda_j\bar{Q}_{jk} \\ &+ (a_{11}a_{33}ch_{jk}^{(1)}sh_{jk}^{(3)} - a_{13}a_{31}sh_{jk}^{(1)}ch_{jk}^{(3)})\mu_k\bar{Q}_{jk}\}, \end{aligned} \tag{29}$$

$$\begin{aligned} D_{jk}^{(3)} = \frac{1}{det_2}\{&(a_{11}a_{22} - a_{12}a_{21})ch_{jk}^{(1)}ch_{jk}^{(2)}\bar{S}_{jk} - (a_{21}a_{32}ch_{jk}^{(1)}sh_{jk}^{(2)} - a_{22}a_{31}sh_{jk}^{(1)}ch_{jk}^{(2)})\lambda_j\bar{Q}_{jk} \\ &+ (a_{11}a_{32}ch_{jk}^{(1)}sh_{jk}^{(2)} - a_{12}a_{31}sh_{jk}^{(1)}ch_{jk}^{(2)})\mu_k\bar{Q}_{jk}\}, \end{aligned} \tag{30}$$

where

$$sh_{jk}^{(i)} \equiv \sinh\frac{\rho_{jk}^{(i)}t}{2} = \sinh\frac{\pi\theta\hat{\rho}_{jk}^{(i)}}{2} \quad , \quad ch_{jk}^{(i)} \equiv \cosh\frac{\rho_{jk}^{(i)}t}{2} = \cosh\frac{\pi\theta\hat{\rho}_{jk}^{(i)}}{2} \quad , \tag{31}$$

$$a_{1i} \equiv \rho_{jk}^{(i)}\frac{A_{31}^{(i)}}{A_{33}^{(i)}} + \lambda_j \quad , \quad a_{2i} \equiv \rho_{jk}^{(i)}\frac{A_{32}^{(i)}}{A_{33}^{(i)}} + \mu_k \quad , \quad a_{3i} \equiv \hat{C}_{zz}\rho_{jk}^{(i)} - \hat{C}_{xz}\frac{A_{31}^{(i)}}{A_{33}^{(i)}}\lambda_j - \hat{C}_{yz}\frac{A_{32}^{(i)}}{A_{33}^{(i)}}\mu_k \quad , \tag{32}$$

$$\bar{Q}_{jk} \equiv \frac{\tilde{N}\bar{P}_{jk}^{(0)}}{E_x t_3 \kappa_{jk}^{\ 2}} \quad , \quad \bar{R}_{jk} \equiv \frac{\tilde{N}}{2E_x}(\bar{P}_{jk}^{(2)} - \bar{P}_{jk}^{(1)}) \quad , \quad \bar{S}_{jk} \equiv \frac{\tilde{N}}{2E_x}(\bar{P}_{jk}^{(1)} + \bar{P}_{jk}^{(2)}) \quad , \tag{33}$$

$$\begin{aligned} det_1 \equiv\ & (a_{12}a_{23} - a_{13}a_{22})a_{31}sh_{jk}^{(2)}sh_{jk}^{(3)}ch_{jk}^{(1)} - (a_{11}a_{23} - a_{13}a_{21})a_{32}sh_{jk}^{(3)}sh_{jk}^{(1)}ch_{jk}^{(2)} \\ & + (a_{11}a_{22} - a_{12}a_{21})a_{33}sh_{jk}^{(1)}sh_{jk}^{(2)}ch_{jk}^{(3)} \quad , \end{aligned} \tag{34}$$

$$\begin{aligned} det_2 \equiv\ & (a_{12}a_{23} - a_{13}a_{22})a_{31}ch_{jk}^{(2)}ch_{jk}^{(3)}sh_{jk}^{(1)} - (a_{11}a_{23} - a_{13}a_{21})a_{32}ch_{jk}^{(3)}ch_{jk}^{(1)}sh_{jk}^{(2)} \\ & + (a_{11}a_{22} - a_{12}a_{21})a_{33}ch_{jk}^{(1)}ch_{jk}^{(2)}sh_{jk}^{(3)} \quad . \end{aligned} \tag{35}$$

In addition, the lateral loads of plates $\bar{p}_i(x,y)$ $(i = 0 \sim 2)$, which include the body force, are assumed to be expanded into Fourier double series as

$$\bar{p}_i(x,y) = \sum_j\sum_k \bar{P}_{jk}^{(i)} \sin\lambda_j x \sin\mu_k y \quad ; \quad \bar{P}_{jk}^{(i)} = \frac{4}{ab}\int_0^b\int_0^a \bar{p}_i(x,y)\sin\lambda_j x \sin\mu_k y dx dy. \tag{36}$$

4. NUMERICAL EXAMPLES

Numerical results of three-dimensional analyses of orthotropic plates will be presented here in order to illustrate validity of the present EFGM. The numerical examples presented here are bending behaviors of rectangular plates under lateral loads, in which the surface traction and the body force are distinguished clearly. The validity of the present procedure can be confirmed by comparing the results of the EFGM with the results of the Fourier analysis.

4.1. Numerical Model

As a numerical model, we adopt here a simply supported rectangular plate as shown in Fig. 2. Mechanical properties of the plate model are as follows: an aspect ratio b/a is 1.0 ; a width-thickness ratio t/a is 0.5 ; Young's modulus ratios are $\alpha_x = 1.0$, $\alpha_y = 2.0$, $\alpha_z = 2.0$ (CASE 1), and $\alpha_z = 3.0$ (CASE 2); shear modulus ratios are $\beta_{xy} = \beta_{zx} = 0.2$ and $\beta_{yz} = 0.8$; Poisson's ratios are $\nu_{xy} = 0.3$, $\nu_{yz} = 0.25$, and $\nu_{zx} = 0.6$.

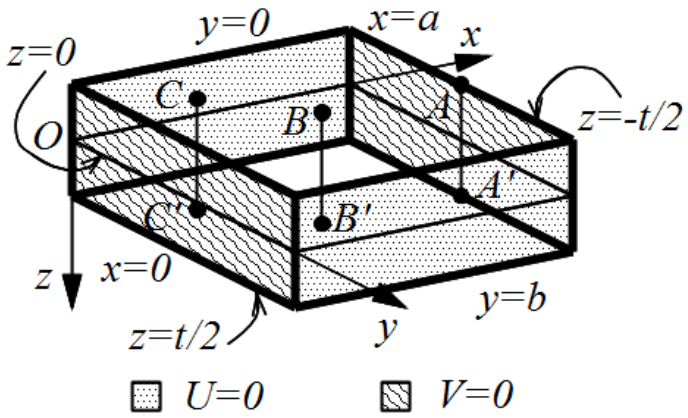

Fig. 2. Simply supported rectangular plate.

Only lateral loads are considered in the present investigation. Two cases of lateral loads are adopted: one is only the surface traction on the upper side as shown in Fig. 3 (Surface Traction Model); the other is only the body force as shown in Fig. 4 (Body Force Model).

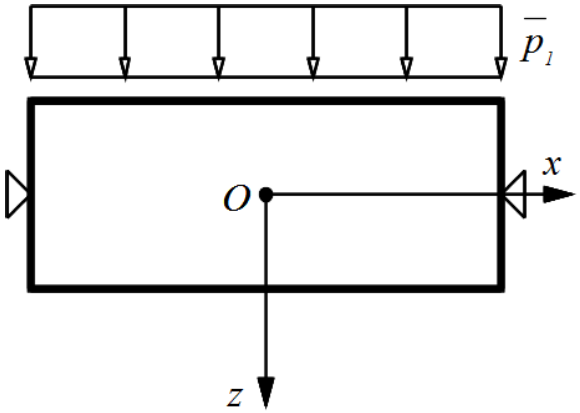

$[\bar{p}_1 = \hat{p}^* \ , \ \bar{p}_0 = 0]$

Fig. 3. Surface traction model.

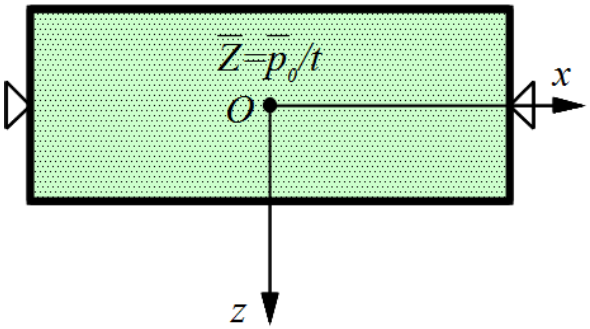

$[\bar{p}_1 = 0 \ , \ \bar{p}_0 = \hat{p}^*]$

Fig. 4. Body force model

Numerical properties in the present EFGM analysis are as follows: total nodes are $11\times11\times11=1331$ which are distributed regularly; number of cells is $5\times5\times5=125$; a support parameter ρ is 0.6; the order of Gaussian quadrature is 5. In the present Fourier analysis, size of the trigonometric series (18) is 150^2.

4.2. Numerical Results

Numerical results are shown in Fig. 5, Fig. 6, and Fig. 7, in which solid lines indicate results of the Fourier analysis and plots results of the EFGM analysis. In those figures, the vertical axis indicates a non-dimensional coordinate along the thickness, $\zeta \equiv z/t$, light-blue lines and red square plots correspond to the results of CASE 1 ($\alpha_z = 2.0$) and brown lines and blue circle plots the results of CASE 2 ($\alpha_z = 3.0$).

Distribution of an in-plane displacement along the line A-A' at $(x, y) = (a, b/2)$ in Fig. 2 is shown in Fig. 5, in which a non-dimensional in-plane displacement $\alpha \equiv U/a$ is depicted against ζ. Figure 5 shows the results of Surface Traction Model. It can be seen from this figure that excellent agreement is achieved between the present EFGM and the Fourier analyses.

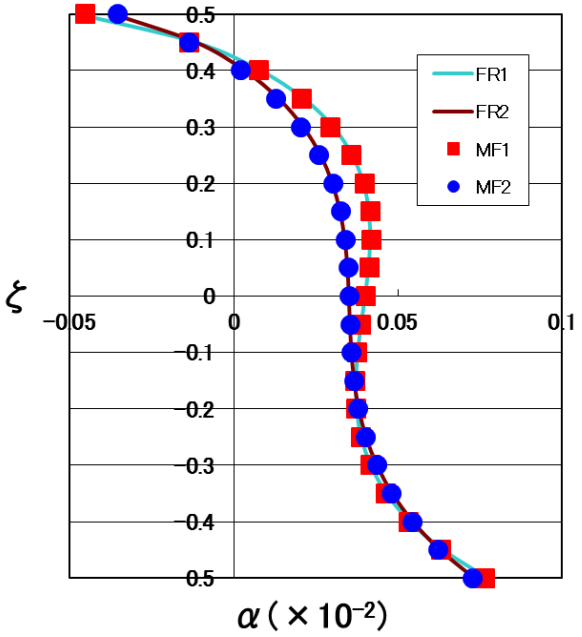

Fig. 5. In-plane displacement distribution

Distribution of a normal stress along the line B-B' at $(x, y) = (a/2, b/2)$ in Fig. 2 is shown in Fig. 6, in which a non-dimensional stress $\sigma^* \equiv (\tilde{N}/E)\sigma_x$ is depicted against ζ. Figure 6 shows the results of Body Force Model. Excellent agreement between the present EFGM and the Fourier analyses can be found again in Fig. 6.

Figure 7 shows distribution of a transverse shear stress of Surface Traction Model along the line C-C' at $(x, y) = (a/4, b/4)$ in Fig. 2. In Fig. 7, a non-dimensional stress $\tau^* \equiv (\tilde{N}/E)\tau_{zx}$ is depicted against ζ. Relatively good approximation is obtained by using the present EFGM. A slight difference, however, is found between two analyses on the results of the transverse shear stress distributions.

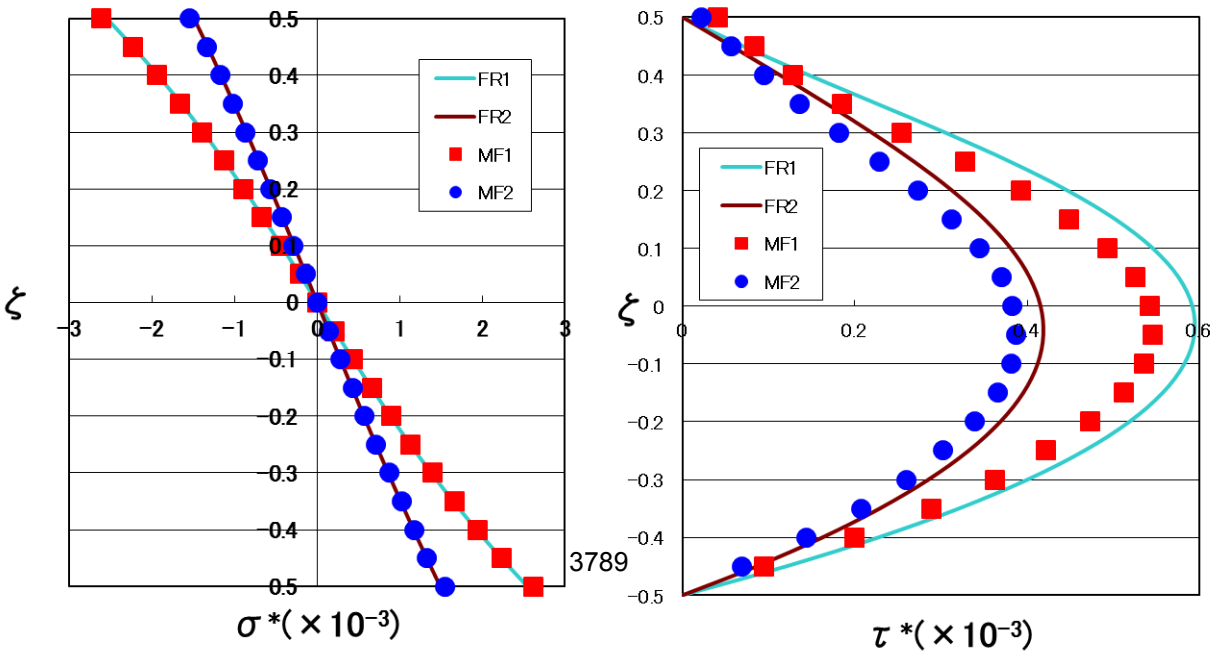

Fig. 6. Normal stress distribution Fig. 7. Transverse shear stress distribution

CONCLUSION

In the present investigation, three-dimensional analyses of orthotropic elastic plates are performed, in which both the element-free Galerkin method and the Fourier analysis are employed. Especially, the present element-free procedure is based on the Lagrange polynomial and, therefore, gives us a quite simple numerical approach. In the Fourier analysis, the body force is also considered, which has been usually ignored in the previous investigations.

Numerical examples demonstrate the validity of the present EFGM for the 3-D analysis orthotropic elastic plates. It follows form the numerical results relatively good approximation is obtained by using the present EFGM. In particular, excellent agreement is achieved between the present EFGM and the Fourier analyses in the results of in-plane displacement and normal stress distributions along the thickness.

REFERENCES

Belytschko, T., Lu, Y.Y., and Gu, L. (1994). "Element-free Galerkin Methods," *Int. J. Numer. Methods Engrg.*, Vol. **37**, 229-256.

Chang, H.-H. and Tarn, J.-Q. (2012). "Three-Dimensional Elasticity Solutions for Rectangular Orthotropic Plates," *J. Elast.,* Vol. **108**, 49-66.

Kaprielian, P.V., Rogers, T.G., and Spencer, A.J.M. (1988). "Theory of Laminated Elastic Plates I. Isotropic Laminae", *Philo. Trans. Roy. Soc. London*, **A324**, 565-594.

Lancaster, P. and Salkauskas, K. (1981). "Surfaces Generated by Moving Least-Squares Methods," *Math. Comput.*, Vol. **37**, 141-158.

Mian, M.A. and Spencer, A.J.M. (1998). "Exact Solutions for Functionally Graded and Laminated Elastic Materials", J. Mech. Phys. of Sol., Vol. **46**(12), 2283-2295.

Nayroles, B., Touzot, G., and Villon, P. (1992). "Generalizing the Finite Element Method: Diffuse Approximation and Diffuse Elements," *Comput. Mech.*, Vol. **10**, 307-318.

Pagano, N.J. (1970). "Exact solutions for rectangular bidirectional composites and sandwich plates," *J. Comp. Mat.,* Vol. **4**, 20-34.

Srinivas, S. and Rao, A.K. (1970). "Bending, vibration and buckling of simply-supported thick orthotropic rectangular plates and laminates," *Int. J. Sol. Struct.,* Vol. **6**, 1463-1481.

Suetake, Y. (2002). "Element-Free Method based on Lagrange Polynomial," *J. Eng. Mech.*, ASCE, Vol. **128**, No.2, 231-239.

Tabakov, P.Y. (2005). “A three-dimensional analysis of laminated orthotropic plates,” *Comp. Struct.,* Vol. **71**(3/4), 453-462.
Wittrick, W. H. (1987). “Analytical, Three-Dimensional Elasticity Solutions to Some Plate Problems, and Some Observation on Mindlin’s Plate Theory”, *Int. J. Sol. Struct.,* Vol. **23**, 441-464.